Materials Chemistry and Physics 144 (2014) 41–48

Contents lists available at ScienceDirect

Materials Chemistry and Physics

journal homepage: www.elsevier.com/locate/matchemphys

Silicone hybrid materials useful for the encapsulation of light-emitting diodes

I-Ann Lei, Dai-Fu Lai, Trong-Ming Don, Wen-Chang Chen, Yang-Yen Yu, Wen-Yen Chiu*

Institute of Polymer Science and Engineering, National Taiwan University, Taipei 10617, Taiwan

HIGHLIGHTS

- Highly stable ZrO_2 particles were synthesized in a commercial-grade silicone material.
- The transmittance of the ZrO_2/silicone hybrid is higher than 95% at wavelength of 400 nm.
- The luminous flux of LEDs was greatly enhanced as encapsulated with the ZrO_2/silicone hybrids.

GRAPHICAL ABSTRACT

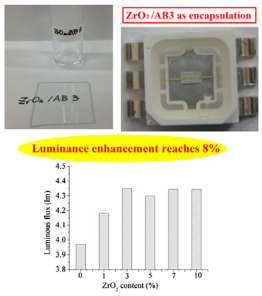

ARTICLE INFO

Article history:
Received 8 July 2013
Received in revised form
1 December 2013
Accepted 8 December 2013

Keywords:
Composite materials
Elastomers
Sol–gel growth
Optical properties

ABSTRACT

Novel ZrO_2/silicone hybrid materials useful for the encapsulation of light-emitting diodes (LEDs) are synthesized by *in situ* sol–gel reaction of zirconium propoxide directly in a commercial-grade silicone resin. The domain size of the produced ZrO_2 particles in the hybrid materials is controlled to be smaller than 350 nm based on SEM pictures to have a high optical transparency greater than 95% at 400 nm. The refractive index of the hybrid material increases from 1.52 to 1.62 when its ZrO_2 content is increased from 1 to 15 wt.%. In addition, these hybrid materials are stable enough to tolerate the treatment of soldering at 260 °C for 2 min. For the hybrid materials with the ZrO_2 content up to 7 wt.%, their weight-loss values are less than 0.25%. Finally, these hybrid materials are applied to encapsulate LEDs and their luminous flux is measured. The results showed that all the hybrid materials have higher luminous flux than the pristine silicone material. The luminous flux increased to a plateau value of 4.35 lm as the ZrO_2 content in the hybrid material was increased to 3.0 wt.%. For all the hybrid materials studied here, the ZrO_2/AB3 hybrid is considered to be the most suitable candidate as the encapsulating material for the LED used in this study.

1. Introduction

In recent years, light emitting diodes (LEDs) have attracted considerable attention due to their increasing applications such as back-light source in the liquid-crystal display, portable light sources and traffic signals [1]. However, one of the limitations in the light extraction efficiency of LEDs is that some of the light could be trapped within the blue chip (light emitter) made from ganium nitrides with a refractive index of 2.6 [2,3], because of the difference in refractive index between the blue chip and air [4–8]. By applying an encapsulating material in the LED housing, the light extraction efficiency can be improved to some extent, in addition to the protection of the device from dust and moisture. Generally, the refractive index of an encapsulating material is between 1.4 and 1.5.

* Corresponding author.
E-mail address: ycchiu@ntu.edu.tw (W.-Y. Chiu).

0254-0584/$ – see front matter © 2013 Elsevier B.V. All rights reserved.
http://dx.doi.org/10.1016/j.matchemphys.2013.12.009

Therefore, the encapsulating material could reduce the refractive index contrast and thus increase the light extraction [9]. There are two types of encapsulating materials, namely, epoxy- and silicone-based encapsulating materials. Compared to the silicone-based materials, the epoxy-based materials have better mechanical properties and thermal stability to the LED housing. However, during the in-device test of LEDs, yellowing of the epoxy-based materials is generally observed in the long-term exposure of blue light which can induce a large amount of heat generated by LEDs. On the other hand, silicone-based encapsulating materials have several advantages such as controlled refractive index, tunable hardness, highly optical transparency in the UV–visible region, and particularly excellent thermal stability against yellowing in the long-term exposure of UV light [10,11]. The hardness and the refractive index can be tuned by changing the organic substituent on the silicon atom of the silicone material. For example, replacing the organic substituent from methyl to phenyl group can increase the refractive index of silicone material from 1.40 to 1.50, and the hardness from shore A to shore D. With all these advantages, the silicone-based resins have thus attracted much attention in the LEDs for the use as the encapsulating material. However, the refractive index of a blue chip is as high as 2.6, much larger than the silicone-based material. According to the Snell's law [12], it is easy to undergo a total internal reflection at the interface between a LED light emitter and the encapsulating material. In order to reduce the total internal reflection and further increase the light extraction coefficient of LEDs, materials with high refractive index are thus exploited. The most common method is introducing inorganic nanoparticles with a high refractive index value to the organic material, thus producing an inorganic/organic hybrid encapsulating material.

Inorganic/organic hybrid materials can be produced by introducing a variety of inorganic additives into the polymer matrix. They have potential applications in many fields as abrasive-resistant coatings, broadband interference filters, and electronic and optical materials [13,14]. However, to achieve the desired properties such as toughness, flexibility, high refractive index and high transparency in the visible region, it is believed that strong interfacial bonding between the organic matrix and the dispersed inorganic particles is required, which can be obtained by modifying the inorganic fillers with appropriate functional groups [15–24]. Alternatively, organic polymers with functional groups, such as carbonyl, hydroxyl and carboxyl groups, can have hydrogen bonding with the inorganic oxide fillers. Among all the methods to produce inorganic/organic hybrid materials, a simple and convenient method is *in situ* polymerization of metal alkoxide compounds directly in the organic polymer matrix. In addition, hybrid materials with uniform-dispersed particles can also be obtained by this method [25–32]. It has been proved that the reaction rate of the *in situ* polymerization is generally governed by the concentration of metal alkoxide, pH value of the medium, type of solvent, and temperature, whereas the particle size of inorganic particles depends on the type and concentration of metal alkoxide, pH value and the interactions between the inorganic oxide and polymer networks [33,34].

In this work, encapsulating hybrid resins with high refractive index were produced by *in situ* formation of zirconium dioxide (ZrO_2) nanoparticles directly in a commercial-grade silicone resin via a sol–gel reaction. The optical transparency of the prepared ZrO_2/silicone resins before and after cure was investigated by UV–visible spectroscopy. In addition to the refractive index, thermal stability of the cured hybrid materials was also investigated in order to meet the requirements of an encapsulating material used for LEDs. Finally, the in-device test was carried out to examine the luminous flux enhancement of these ZrO_2/silicone hybrid materials.

2. Experimental

2.1. Materials

Zirconium propoxide (ZPP), 1-butanol (BuOH), methyl ethyl ketone (MEK), 2,4-pentanedione, and tetrahydrofuran (THF) were purchased from Acros Organics. Acetic acid (AcOH) was supplied from Fisher Chemical. A commercial-grade encapsulating material based on silicone resin, OE-6630 from Dow Corning, was used in this study. It was supplied as a two-part A/B kit. The A-part as a base resin contained dimethylvinylsiloxy-terminated methylphenyl siloxane, phenylmethyl cyclosiloxane, silicone resin and catalyst. It had a viscosity of 2975 mPa s. The B-part was mainly composed of silsesquioxane and polysiloxane. Its viscosity was 2775 mPa s [35]. All materials were used without any further purification.

2.2. Synthesis of zirconium dioxide via sol–gel reaction in the A part resin

Specific amounts of ZPP and AcOH as well as 1 g A-part resin were first added to a solution composed of equal weights of MEK and BuOH. When a certain amount of deionized water was added to initiate the sol–gel reaction, the solution was immediately sonicated with an ultrasonicator (50 W, 30 KHz, 100% amplitude output, Dr. Hielscher UP-50H) in an ice-bath. Two different sonication times were adopted, where 1 min was applied to the solutions with lower ZPP amounts and 30 min were applied to those with higher ZPP amounts. For all systems, the molar ratios of the ZPP to the AcOH and to the water were both fixed at 1/2, and a sufficient amount of MEK/BuOH was added to maintain a constant ZPP concentration in the solution at 13.3 wt.%. Subsequently, the B-part resin (1 g) was added into the solution. The solution was heated at 70 °C in a rotary evaporator to remove the solvents until the sample weight was unchanged. It was then mixed with 2,4-pentanedione with a molar amount equal to the original ZPP to prevent from aggregation of ZrO_2 particles [36–38], and stored at 4 °C. The recipes for preparing these ZrO_2/AB resins with different weight fractions of ZrO_2 are listed in Table 1.

2.3. Curing of AB and ZrO_2/AB resins

For comparison, pure silicone resin was also prepared by directly mixing the A-part and B-part resins with equal amounts. Sample films were prepared for measuring their optical and thermal properties according to the following procedure. All the AB and ZrO_2/AB resins were diluted with THF to a concentration of 10 wt.%, and poured into a Teflon mold or dropped onto a glass slide. They were subsequently cured at 80 °C for 30 min, and then 150 °C for 1 h to obtain the crosslinked ZrO_2/AB hybrid films.

3. Characterizations

Surface morphology of the ZrO_2/AB films and the size of the dispersed ZrO_2 particles were examined by using a scanning electron microscope (Nova NanoSEM 230).

The transmittances of the ZrO_2/AB resins before and after cure were measured by a UV–visible spectrophotometer (model HeλIOSγ, Thermo Spectronic Co., USA) from 300 nm to 800 nm in the wavelength.

Thermal degradation behavior of the cured ZrO_2/AB resins was studied by a thermo-gravimetric analyzer (Pyris TGA7, Perkin–Elmer, USA) from 110 °C to 800 °C with a heating rate of 10 °C min^{-1} under a N_2 atmosphere, where the ZrO_2/AB hybrids were pre-dried at 100 °C for 24 h. In addition, the thermal stability of the ZrO_2/AB hybrids was further examined by heating them at 260 °C for 5 min.

Table 1
Recipes for synthesizing the ZrO_2/AB with different ZrO_2 contents.

Sample	ZPP[a] [g]	A [g]	B [g]	AcOH [g]	Water [g]	MEK/BuOH [1/1] [g]	Sonication time [min]	ω_{ZrO2}[b] [wt.%]
ZrO_2/AB1	0.053	1.00	1.00	0.020	0.006	0.325	1	1
ZrO_2/AB3	0.162	1.00	1.00	0.060	0.018	0.975	1	3
ZrO_2/AB5	0.285	1.00	1.00	0.100	0.030	1.710	1	5
ZrO_2/AB7	0.403	1.00	1.00	0.140	0.042	2.430	30	7
ZrO_2/AB10	0.596	1.00	1.00	0.200	0.060	3.580	30	10
ZrO_2/AB15	0.940	1.00	1.00	0.300	0.090	5.670	30	15

[a] The molar ratios of [ZPP]/[AcOH] and [ZPP]/[H_2O] were both set at 1/2. The ZPP concentration in the sol–gel reaction solution was maintained at 13.3 wt.% by adding a sufficient amount of MEK/BuOH.
[b] The theoretical weight percentage of ZrO_2 (ω_{ZrO2}) in the final ZrO_2/AB hybrid was calculated by assuming that all ZPP was completely converted to ZrO_2 after sol–gel reaction, $\omega_{ZrO2} = W_{ZrO2}/(W_{ZrO2} + W_{AB}) \times 100$.

The refractive index of the cured ZrO_2/AB films was determined by ellipsometry (GES 5E variable-angle spectroscopic ellipsometer, Sopra Inc., USA) in the wavelength range from 300 nm to 800 nm.

The in-device test was carried out to examine the luminous flux enhancement of the prepared ZrO_2/AB resins. High-power LEDs of Blue chip (20 × 38 mil, V20A, Epistar Corp., Taiwan) were encapsulated with the ZrO_2/AB resins by applying them into the LED assembly. They were cured at 80 °C for 30 min, 90 °C for 3 h, 110 °C for 30 min, and finally 150 °C for 1 h. The light-emitting characteristic of the LEDs in terms of lumen output with a power supply of 150 mA and 5 V was measured at room temperature on a CAS-140B compact array spectrometer (Instrument Systems GmbH).

4. Results and discussion

4.1. Particle size of ZrO_2 in the ZrO_2/AB hybrids

In this study, ZrO_2 nanoparticles were synthesized by an *in situ* sol–gel reaction of ZPP mainly in the A-part silicone resin of a commercial-grade encapsulating material. The sol–gel reaction of the ZPP in the A-part resin was initiated by the addition of water. They were then mixed with the B-part resin to form the hybrid ZrO_2/AB resins. It is known that the size of the inorganic particles produced by sol–gel reaction is strongly dependent on the type and concentration of metal alkoxide, addition of chelating agent, pH value of medium, the type of solvent, and agitation [33,34]. In the present study, these factors were all considered simultaneously to control the ZrO_2 particle size during the sol–gel reaction. First, acetic acid was used as a chelating agent for the ZPP that would inhibit the particle growth. It could also provide a low pH environment that would increase the hydrolysis reaction and decrease the condensation reaction. Consequently, more nucleating sites are created with a result of smaller ZrO_2. In the mean time, acetic acid is able to modify the surface of ZrO_2 particles for providing the interfacial bonding with the silicon resin [39,40]. Secondly, various kinds of solvent and mix solvent, which are compatible with AB resin, were employed into the synthesis. It was found that MEK/BuOH mix solvent was able to control the growing rate also to retard mutual aggregation among ZrO_2 nanoparticles (see Supporting information Table 1S.). In the literature [36–38,41,42], it is reported that the hydroxyl and carbonyl groups are able to retard the gelation rate of the metal alkoxide compound as well as the growing rate of ZrO_2. The mixed MEK/BuOH solvent was therefore selected not only to maintain a constant concentration of the ZPP in all systems but also to control the growing rate of ZrO_2 in the reaction solution. Finally, an ultrasonication was applied to further prevent the aggregation of the produced ZrO_2 particles during the sol–gel reaction. It was found that increasing the sonication time increased the dispersion and decreased the particle size of the ZrO_2 in the resin. Our results shows that 1 min of sonication is enough to prevent the aggregation of ZrO_2 particles for the systems with lower ZrO_2 content, yet not enough for those with the ZrO_2 content higher than 5 wt.%. To ensure the ZrO_2/AB hybrid materials with high optical transparency, the sonication time was increased to 30 min for the systems of ZrO_2/AB7 to ZrO_2/AB15.

The A-part resin consists of a platinum complex as catalyst and vinyl-terminated dimethylsiloxane oligomer, whereas the B-part resin is an alkylhydrosiloxane oligomer used as a crosslinker. When the A-part and B-part resins are mixed together, heated at 80 °C for 30 min and cured at 150 °C for 1 h, hydrosilation reaction occurs as Equation (1).

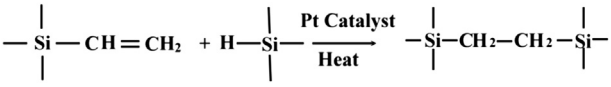

(1)

Then we obtained the crosslinked ZrO_2/AB hybrid materials. The surface morphology of the ZrO_2/AB hybrid films was then revealed by a scanning electronic microscope as shown in Fig. 1. As mentioned previously, Fig. 1 shows that the ZrO_2/AB7 system has the smallest particle size among all systems studied here. The ultrasonication are therefore proved to be capable of disrupting the particle aggregates very well. In addition, comparing the group of ZrO_2/AB1 to ZrO_2/AB5 with the group of ZrO_2/AB7 to ZrO_2/AB15 films, it can be deduced that the increase of sonication time leads to a more uniform particle size distribution and higher dispersion as well as a decrease in the particle size of ZrO_2. However, the dispersed particles in the films became larger than those in the resins before cure. It is believed that the sol–gel reaction continues during the curing process at high temperatures, especially the condensation reaction, thereby increasing the particle size of ZrO_2. It is also possible that the aggregation of ZrO_2 particles becomes more obvious due to the crosslinking of the silicone elastomer. Still, the average particle size is smaller than 350 nm for all the systems studied here except the ZrO_2/AB15 with the highest ZrO_2 content.

4.2. Transmittance of the ZrO_2/AB hybrid materials

The transmittance of various ZrO_2/AB resins before and after cure was measured by a UV–visible spectrophotometer in the wavelength range from 300 nm to 800 nm. Except the ZrO_2/AB15 resin with the highest ZrO_2 content, Fig. 2 shows that all the ZrO_2/AB resin solutions before cure are transparent in the wavelength region of visible light, and their transmittance values are all greater than 93% at the wavelength of 400 nm. Compared with the pristine AB resin, the introduction of ZrO_2 causes an absorption in the wavelength range from 300 nm to 400 nm, and the absorption becomes more evident with an increase in the ZrO_2 content. It was reported that the amorphous zirconia has an absorption in the near ultraviolet range [43]. Moreover, a shoulder in the wavelength

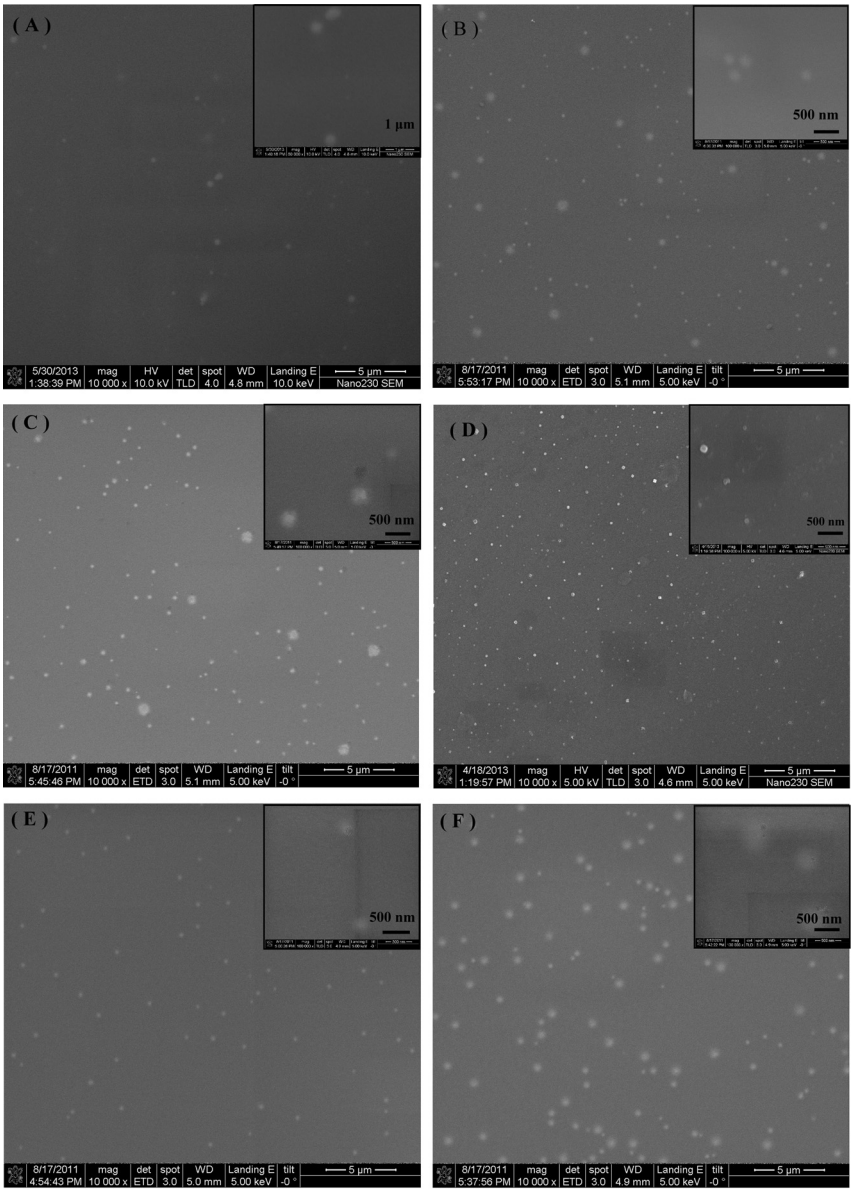

Fig. 1. Surface morphology of the cured ZrO_2/AB films (A) ZrO_2/AB1[a] (=0.35 ± 0.13 μm), (B) ZrO_2/AB3 (=0.28 ± 0.11 μm), (C) ZrO_2/AB5 (=0.19 ± 0.05 μm), (D) ZrO_2/AB7 (=0.16 ± 0.05 μm), (E) ZrO_2/AB10 (=0.34 ± 0.06 μm), (F) ZrO_2/AB15 (=0.47 ± 0.11 μm). The value is the average ZrO_2 domain size based on 50 particles.

range from 335 nm to 380 nm was revealed in the spectra of ZrO_2/AB resins. This is due to the coordination of the acetic acid to the zirconia [44], suggesting that some residual chelating acetic acid on the zirconia remains in the ZrO_2/AB resins even after evaporation of the solvents. This also explains that the ZrO_2/AB15 resin appears to be slightly yellowish and its transmittance is lower than 85% at the wavelength of 400 nm.

After the cure of the hybrid ZrO_2/AB resins at high temperatures, Fig. 3 shows that all the transmittance values of the hybrid films, except the one with the highest ZrO_2 content, are greater than 95% at the wavelength of 400 nm. The results were summarized in Table 2. In addition, the absorption in the near ultraviolet region indicated that the produced zirconia was amorphous and confirmed by the XRD analysis. Generally, the diffraction peaks of the ZrO_2 with crystal structures exist at 28° and 30° in 2θ [45]. However, we did not observe any peak appearing in the 2θ angle ranging from 20° to 80° in the ZrO_2/AB hybrids (see Supporting information Fig. 1S). Compared to the resin solutions before cure in Fig. 2, the absorption in the wavelength range from 335 nm to 380 nm due to the coordination of the acetic acid to the zirconia was found to be much less for the cured ZrO_2/AB films. It is reasonable to assume that most chelating acetic acid is evaporated during the cure at high temperatures. In summary, the high transparency of the ZrO_2/AB hybrid materials before and after cure is attributed to the well-dispersed ZrO_2 nanoparticles achieved by using the chelating agent of acetic acid, the cosolvents and ultrasonication.

In addition, the transmittance of the cured hybrid ZrO_2/AB resin in the range from 380 nm to 780 nm was transferred into the yellowness index [46] to estimate the degree of yellowing after introducing the ZrO_2 particles into the silicone material, and the results were summarized in Table 2. As shown in Table 2, the yellowness index of the AB cured film is 0.25. After incorporation of ZrO_2, the yellowness index increased from 0.25 for the AB cured

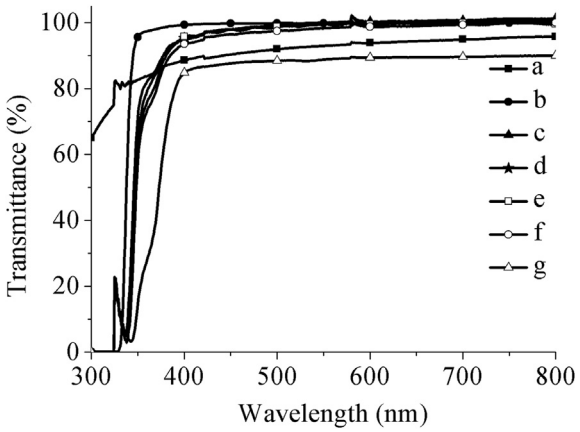

Fig. 2. Transmittance of the AB and ZrO_2/AB resins before cure (path length = 1 mm): (a) AB, (b) ZrO_2/AB1, (c) ZrO_2/AB3, (d) ZrO_2/AB5, (e) ZrO_2/AB7, (f) ZrO_2/AB10, (g) ZrO_2/AB15.

film to 2.23 for the ZrO_2/AB15 cured film with the highest ZrO_2 content. Though incorporation of ZrO_2 would cause the yellowing of the silicone material, the degree of yellowing is not high owing to the well-dispersed ZrO_2 particles in the ZrO_2/AB hybrid films.

4.2.1. *Thermal degradation and stability of the ZrO_2/AB hybrid materials*

Thermal degradation of the produced ZrO_2/AB hybrid materials was studied by a thermo-gravimetric analyzer, in which the weight loss of sample was recorded during the heating process as shown in Fig. 4. It can be seen that all the ZrO_2/AB hybrid materials degraded earlier than the pure silicone material. The onset degradation temperatures (T_{onset}, the temperature at 1 wt.% loss) of various ZrO_2/AB materials were summarized in Table 2, where the T_{onset} decreased from 343 °C for the pure AB elastomer to 208 °C for the ZrO_2/AB15 hybrid with the highest content of ZrO_2. There are three possible reasons for the decrease of the onset degradation temperature: (1) the physical hindrance imparted by ZrO_2 particles retards the curing reaction and thereby lowered the crosslinking density [47]. It was confirmed by the DSC analysis of the pure AB and the ZrO_2/AB resins, and the hardness measurement of the pure AB silicone and the ZrO_2/AB hybrids with the thickness of 1 cm. From the results of the DSC analysis, the reaction heat of the

Table 2
Thermal and optical properties of the cured AB and ZrO_2/AB films.

Sample	Refractive index (n)[a]	T (%) at 400 nm	Yellowness index (Y.I.)	T_{onset}[c] (°C)	Weight loss (%) at 260 °C for 2 min
AB	1.502	98.9 (0.93 μm)[b]	0.25	343	0.046
ZrO_2/AB1	1.520	97.5 (1.44 μm)	0.86	334	0.111
ZrO_2/AB3	1.537	97.6 (1.49 μm)	0.76	287	0.227
ZrO_2/AB5	1.573	98.4 (1.55 μm)	0.65	276	0.232
ZrO_2/AB7	1.578	96.9 (0.95 μm)	0.87	232	0.232
ZrO_2/AB10	1.592	95.9 (0.84 μm)	1.01	232	0.384
ZrO_2/AB15	1.620	88.2 (1.35 μm)	2.23	208	0.494

[a] The refractive index was determined at the wavelength of 633 nm.
[b] The value in the parenthesis is the thickness of the film.
[c] T_{onset} is the onset degradation temperature at 1 wt.% loss of sample.

silicone resin was gradually decreased with increasing the weight percentage of the ZrO_2 in the ZrO_2/AB resins (see Supporting information Table 2S.). The results of the shore hardness measurement also show that the hardness was decreased from shore A 56 (for the pure AB elastomer) to shore A 50 (for the ZrO_2/AB3 hybrid) after incorporation of the ZrO_2 particles (see Supporting information Table 3S.). Thus, it could be concluded that the crosslinking density of the silicone material is lowered by introducing the ZrO_2 particles, and it is generally believed that the lower crosslinking density can cause a lower onset degradation temperature. (2) The residual substances left in the hybrid materials such as the chelating acetic acid and residual solvents lead to the earlier weight-loss of these hybrid materials. Since the added amounts of the acetic acid and solvents are proportional to the addition of ZPP. (3) The further condensation reaction of ZrO_2 accompanied with water by-product during the heating process in the TGA experiment leads to the further weight loss of these hybrids materials. For the above reasons, the T_{onset} thus decreases gradually with increasing the ZrO_2 content in the ZrO_2/AB hybrid materials.

Fig. 4 also shows that the weight loss of the ZrO_2/AB hybrid is postponed in the temperature range from 300 °C to 600 °C. Unlike the T_{onset}, it is revealed that the thermal resistance of the ZrO_2/AB hybrids was increased greatly after incorporation of ZrO_2 particles. Similar behaviors have been reported in numerous studies that the introduction of inorganic particles in polymer matrix could improve the thermal stability of the hybrids [48,49]. They attributed the increase in the thermal resistance to the intrinsic thermal stability of inorganic particles. Compared to the group of ZrO_2/AB1 to ZrO_2/AB5, the enhancement in the thermal resistance is not so

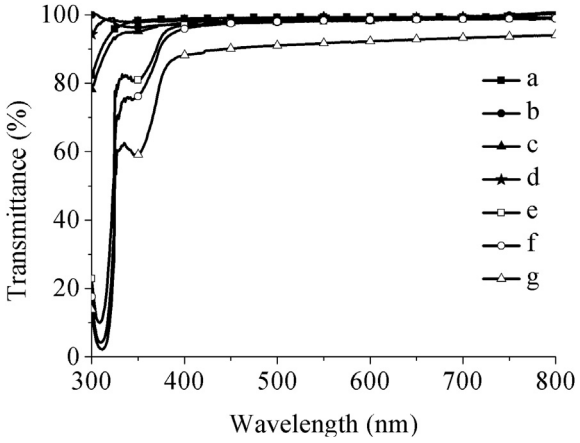

Fig. 3. Transmittance of the cured AB and ZrO_2/AB films: (a) AB, (b) ZrO_2/AB1, (c) ZrO_2/AB3, (d) ZrO_2/AB5, (e) ZrO_2/AB7, (f) ZrO_2/AB10, (g) ZrO_2/AB15 (The film thickness was in the range of 0.84–1.55 μm as listed in Table 2.).

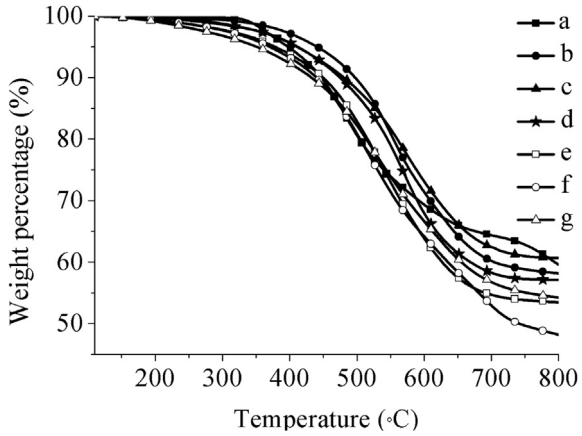

Fig. 4. Thermal degradation curves of the cured AB and ZrO_2/AB resins: (a) AB, (b) ZrO_2/AB1, (c) ZrO_2/AB3, (d) ZrO_2/AB5, (e) ZrO_2/AB7, (f) ZrO_2/AB10, (g) ZrO_2/AB15.

significant for the group of ZrO_2/AB7 to ZrO_2/AB15. As mentioned previously, the incorporation of ZrO_2 particles would lower the crosslinking density of the silicone material, thus, despite of more ZrO_2 particles exist in the group of ZrO_2/AB7 to ZrO_2/AB15 hybrids, the improvement in the thermal resistance is limited.

After encapsulation, the LED must be exposed to lead-free solder temperature of 260 °C for 2 min in the surface mount technology (SMT) which is expected to become the manufacturing norm for LED assemblies. The encapsulating material is thus required to be thermally stable at 260 °C for at least 2 min. Though Table 2 already shows that the onset degradation temperatures of all encapsulating materials with the final ZrO_2 contents up to 5 wt.% are greater than 260 °C, it is still important to know their thermal stability at 260 °C with time. All the samples were thus kept at 260 °C for 5 min and the weight loss was recorded. The weight loss was found to increase with time as shown in Fig. 5. In addition, the ZrO_2/AB hybrids had a higher weight loss than the pure AB silicone material as the same situation observed in the trend of onset degradation temperature. The data of the weight loss of various samples at 260 °C for 2 min were summarized in Table 2. The weight loss is 0.046% for the pure silicone material and then increases slowly with increasing the ZrO_2 content in the hybrid material. Still, the weight loss is considered very small and the majority of the sample is still retained. For the hybrid materials with the final ZrO_2 content up to 7 wt.%, the weight-loss values are less than 0.25%, indicating these hybrid materials are stable enough to tolerate the treatment of soldering the LED on the printed circuit board at 260 °C for 2 min.

4.2.2. Refractive index of the ZrO_2/AB hybrid materials

The refractive index of the pure AB elastomer and the ZrO_2/AB hybrid materials was determined by an ellipsometer in the wavelength range from 250 nm to 800 nm. Fig. 6 shows that the introduction of the high-refractive-index ZrO_2 into the silicone material could effectively increase the refractive index of the encapsulating material. The values at the wavelength of 633 nm were summarized in Table 2. The refractive index of the pure AB silicone material is 1.502 at 633 nm. As explained previously in the UV–visible spectra of the ZrO_2/AB hybrids, the produced ZrO_2 particles are amorphous. A value of 1.80 is thus taken for the amorphous ZrO_2 synthesized by a sol–gel reaction [49]. The refractive index at 633 nm was increased to 1.520 for the ZrO_2/AB1 hybrid with only 1 wt.% ZrO_2; it then gradually increased with increasing the ZrO_2 content. The value was increased to 1.620 for the ZrO_2/AB15 with the highest ZrO_2 content of 15 wt.%. Generally, the higher the refractive index of the encapsulating material, the smaller the difference in the refractive indices between the encapsulating material and the blue chip of LEDs. Consequently, the Fresnell loss can be reduced.

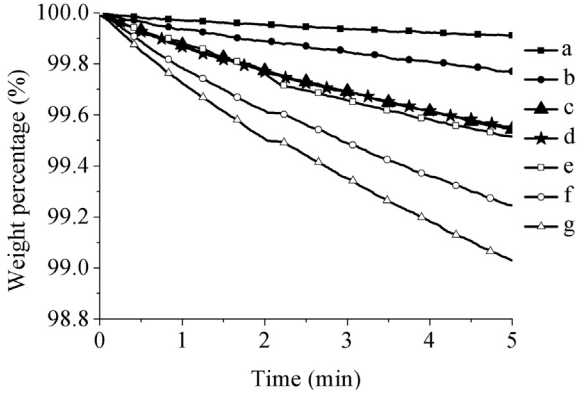

Fig. 5. Thermal stability of the cured AB and ZrO_2/AB resins at 260 °C: (a) AB, (b) ZrO_2/AB1, (c) ZrO_2/AB3, (d) ZrO_2/AB5, (e) ZrO_2/AB7, (f) ZrO_2/AB10, (g) ZrO_2/AB15.

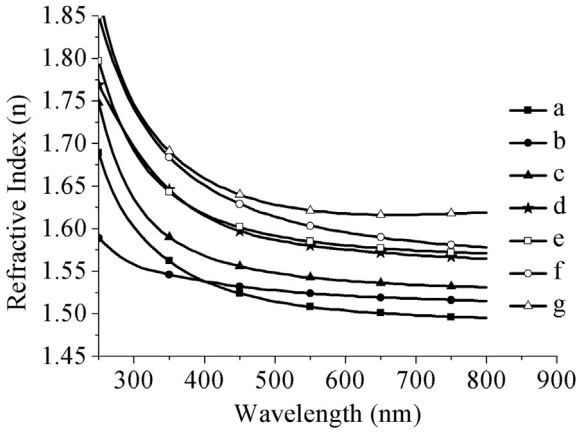

Fig. 6. Refractive index of the cured AB and ZrO_2/AB films: (a) AB, (b) ZrO_2/AB1, (c) ZrO_2/AB3, (d) ZrO_2/AB5, (e) ZrO_2/AB7, (f) ZrO_2/AB10, (g) ZrO_2/AB15.

4.2.3. Luminous flux of LEDs encapsulated with the ZrO_2/AB hybrid materials

Introducing ZrO_2 into the silicone material leads to an increase in the refractive index. These high-refractive-index hybrid materials were then used as encapsulating materials for LEDs to improve the extraction coefficient of light emitted from LEDs. Before encapsulation, the luminous flux of a bare LED was measured in the wavelength range from 380 to 780 nm and found to be 3.85. After encapsulation with the pure AB silicone material on the LED, the luminous flux was increased to 3.97. By using the ZrO_2/AB hybrids as encapsulating materials, the luminous flux of LED was greatly enhanced, because the ZrO_2/AB hybrids had higher refractive index than the pure AB silicone material. As shown in Fig. 7, a maximum in luminous flux is already achieved at a value of 4.35 for the LED encapsulated with the ZrO_2/AB3. This is because for this particular 20x38 mil chip, a silicon dioxide thin film is fully applied on the chip as a passivation layer to prevent the shortage between the electrodes. Since the refractive index of the silicon dioxide film is about 1.55, the optimum value of refractive index for the encapsulating material should be around 1.55. The excess of the refractive index more than that of the silicon dioxide thin film could cause an increase in the Fresnell loss on interfaces. Among all the ZrO_2/AB hybrids, the ZrO_2/AB3 thus has the closest value of refractive index to the silicon dioxide film. For other types of blue chip, the hybrid

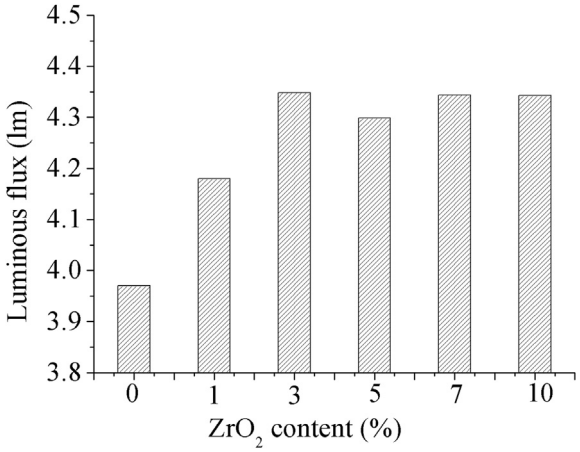

Fig. 7. The effect of ZrO_2 content in the ZrO_2/AB encapsulating material on the luminous flux of the LEDs. The luminous flux of the bare chip without any encapsulation was 3.85 lm.

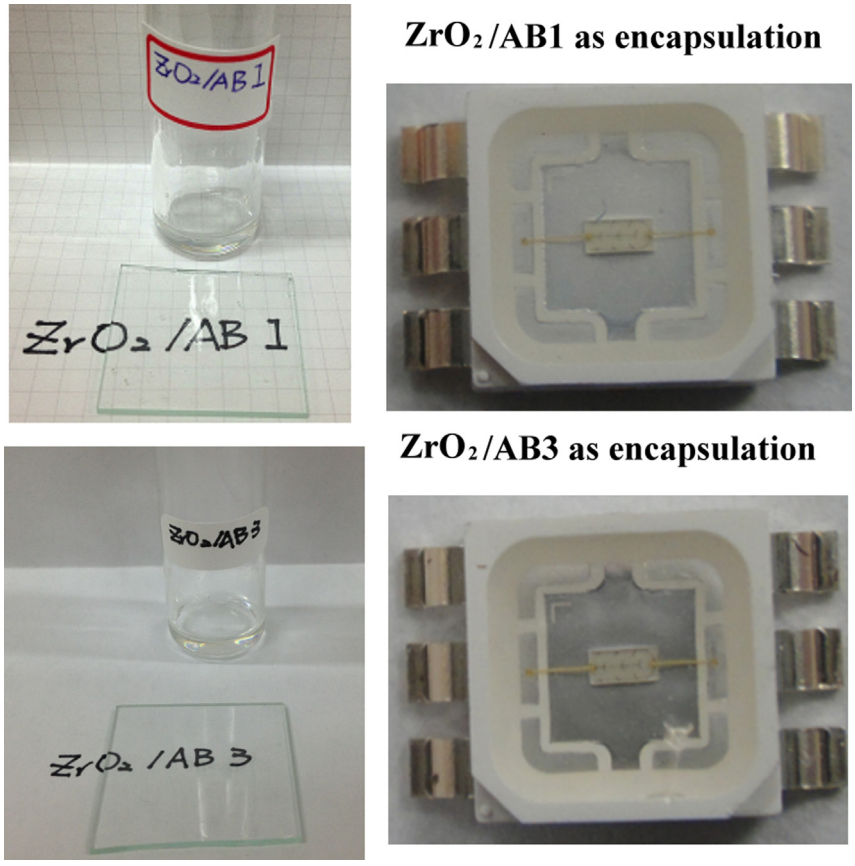

Fig. 8. The photographs of the LEDs encapsulation with the ZrO_2/AB1 and the ZrO_2/AB3 hybrids, and the cured thin films of the ZrO_2/AB1 and ZrO_2/AB3 hybrids.

material with higher ZrO_2 contents might have higher luminous flux. The photographs of the LEDs encapsulated with the ZrO_2/AB1 and the ZrO_2/AB3 hybrid are shown in Fig. 8.

5. Conclusions

High-refractive-index encapsulating materials were fabricated by incorporating ZrO_2 nanoparticles into the silicon resin through an *in situ* sol–gel reaction of zirconium propoxide. By using MEK and BuOH as co-solvent and acetic acid as chelating agent, nano-sized ZrO_2 particles with a high degree of dispersion were produced in the silicone matrix with the help of ultrasonication, thereby resulting in the high transparency of the synthesized encapsulating materials. The thermal stability was satisfactory with only 0.25% in the weight loss at 260 °C for 2 min for the hybrid materials with the ZrO_2 content up to 7 wt.%. Moreover, the luminous flux was increased greatly from 3.97 for the LED encapsulated with the pure AB silicone to a value of 4.35 for the one encapsulated with the ZrO_2/AB3. From all the measured properties, the ZrO_2/AB3 hybrid is considered to be the most suitable candidate as the encapsulating material for the LED used in this study.

Appendix A. Supplementary data

Supplementary data related to this article can be found at http://dx.doi.org/10.1016/j.matchemphys.2013.12.009.

References

[1] A. Gautam, F.C.J.M. van Veggel, ACS Appl. Mater. Interfaces 4 (2012) 3902.
[2] Y. Xi, X. Li, J.K. Kim, F. Mont, T. Gessmann, H. Luo, E.F. Schubert, 4 ed., AVS, vol. 24, 2006, p. 1627.
[3] S. Manna, V.D. Ashok, S.K. De, ACS Appl. Mater. Interfaces 2 (2010) 3539.
[4] F.W. Mont, J.K. Kim, M.F. Schubert, E.F. Schubert, R.W. Siegel, J. Appl. Phys. 103 (8) (2008) 083120.
[5] J.W. Lee, J. Cho, S. Yoon, H. Kim, Y.J. Sung, C. Sone, Y. Park, T.G. Kim, in: Compound Semiconductors 2004, Proceedings, vol. 184, Lop Publishing, Bristol, 2005, p. 333.
[6] A.I. Zhmakin, Phys. Rep. 498 (2011) 189.
[7] K.S. Kim, S.-M. Kim, H. Jeong, M.S. Jeong, G.Y. Jung, Adv. Funct. Mater. 20 (2010) 1076.
[8] B.-U. Ye, B.J. Kim, Y.H. Song, J.H. Son, H. k. Yu, M.H. Kim, J.-L. Lee, J.M. Baik, Adv. Funct. Mater. 22 (2012) 632.
[9] Z. Liu, S. Liu, K. Wang, X. Luo, Front. Optoelectron. 2 (2009) 119.
[10] A.V. Vázquez, A.P. Boughton, N.E. Shephard, S.M. Rhodes, Z. Chen, ACS Appl. Mater. Interfaces 2 (2009) 96.
[11] E. Delebecq, F. Ganachaud, ACS Appl. Mater. Interfaces 4 (2012) 3340.
[12] Y.H. Lin, J.P. You, Y.C. Lin, N.T. Tran, F.G. Shi, IEEE Trans. Compon. Packag. Technol. 33 (2010) 761.
[13] D.F. Cheng, A. Hozumi, ACS Appl. Mater. Interfaces 3 (2011) 2219.
[14] R.A. Zoppi, C.R. de Castro, I.V.P. Yoshida, S.P. Nunes, Polymer 38 (1997) 5705.
[15] K. Bula, T. Jesionowski, A. Krysztafkiewicz, J. Janik, Colloid Polym. Sci. 285 (2007) 1267.
[16] C. Guan, C.L. Lu, Y.F. Liu, B. Yang, J. Appl. Polym. Sci. 102 (2006) 1631.
[17] L.H. Lee, W.C. Chen, Chem. Mater. 13 (2001) 1137.
[18] K.Q. Luo, S.X. Zhou, L.M. Wu, Thin Solid Films 517 (2009) 5974.
[19] K.Q. Luo, S.X. Zhou, L.M. Wu, B. You, Thin Solid Films 518 (2010) 6804.
[20] M. Nakade, K. Kameyama, M. Ogawa, J. Mater. Sci. 39 (2004) 4131.
[21] M. Xiong, S. Zhou, B. You, L. Wu, J. Polym. Sci. Part B: Polym. Phys. 43 (2005) 637.
[22] K. Xu, S. Zhou, L. Wu, Prog. Org. Coat. 67 (2010) 302.
[23] Z.H. Huang, K.Y. Qiu, Polymer 38 (1997) 521.
[24] T. Otsuka, Y. Chujo, Polymer 50 (2009) 3174.
[25] M.J. Arlen, D. Wang, J.D. Jacobs, R. Justice, A. Trionfi, J.W.P. Hsu, D. Schaffer, L.-S. Tan, R.A. Vaia, Macromolecules 41 (2008) 8053.
[26] Y. Gao, N.R. Choudhury, N. Dutta, J. Matisons, M. Reading, L. Delmotte, Chem. Mater. 13 (2001) 3644.
[27] Y. Hu, G. Gu, S. Zhou, L. Wu, Polymer 52 (2011) 122.
[28] Y.Q. Hu, S.X. Zhou, L.M. Wu, Polymer 50 (2009) 3609.

[29] H.-J. Lee, S.-J. Oh, J.-Y. Choi, J.W. Kim, J. Han, L.-S. Tan, J.-B. Baek, Chem. Mater. 17 (2005) 5057.
[30] W.C. Liaw, K.P. Chen, Eur. Polym. J. 43 (2007) 2265.
[31] G. Polizos, E. Tuncer, I. Sauers, K.L. More, Appl. Phys. Lett. 96 (2010).
[32] H. Zeng, C. Gao, Y. Wang, P.C.P. Watts, H. Kong, X. Cui, D. Yan, Polymer 47 (2006) 113.
[33] J. Livage, M. Henry, C. Sanchez, Prog. Solid State Chem. 18 (1988) 259.
[34] E. Matijevic, Chem. Mater. 5 (1993) 412.
[35] Dow Corning(R) OE-6630 A/B KIT, Dow Corning Corporation Material Safety data Sheet, Version: 1.5 Revision Date: 2009/07/10, www.dowcorning.com.
[36] A. Leaustic, F. Babonneau, J. Livage, Chem. Mater. 1 (1989) 240.
[37] A. Yamamoto, S. Kambara, J. Am. Chem. Soc. 79 (1957) 4344.
[38] X. Jiang, T. Herricks, Y. Xia, Adv. Mater. 15 (2003) 1205.
[39] M. Ochi, D. Nii, M. Harada, J. Mater. Sci. 45 (2010) 6159.
[40] M. Ochi, D. Nii, Y. Suzuki, M. Harada, J. Mater. Sci. 45 (2010) 2655.
[41] C. Sanchez, J. Livage, M. Henry, F. Babonneau, J. Non-Cryst. Solids 100 (1988) 65.
[42] A. Vioux, Chem. Mater. 9 (1997) 2292.
[43] N. Yamada, I. Yoshinaga, S. Katayama, J. Sol-Gel Sci. Technol. 17 (2000) 123.
[44] J. Mendez-Vivar, C.J. Brinker, J. Sol-Gel Sci. Technol. 2 (1994) 393.
[45] R. Srinvasan, R.J. De Angelis, G. Ice, B.H. Davis, J. Mater. Res. 6 (1991) 1287.
[46] J.-S. Kim, S. Yang, B.-S. Bae, Chem. Mater. 22 (2010) 3549.
[47] G. Polizos, E. Tuncer, I. Sauers, K.L. More, Polym. Eng. Sci. 51 (1) (2011) 87–93.
[48] K. Kukli, M. Ritala, M. Leskelä, Chem. Vap. Deposition 6 (2000) 297.
[49] N. Nakayama, T. Hayashi, J. Appl. Polym. Sci. 105 (2007) 3662.